Journal of Molecular Spectroscopy **206,** 27–32 (2001)
doi:10.1006/jmsp.2000.8285, available online at http://www.idealibrary.com on IDEAL®

Fourier Transform Emission Spectroscopy of CuCl

T. Parekunnel,* L. C. O'Brien,† T. L. Kellerman,† T. Hirao,* M. Elhanine,‡ and P. F. Bernath*,§

*Department of Chemistry, University of Waterloo, Waterloo, Ontario, Canada N2L 3G1; †Department of Chemistry, Southern Illinois University, Edwardsville, Illinois 62026-1652; ‡Laboratoire de Photophysique Moléculaire du CNRS, Bâtiment 210, Université Paris Sud, 91405 Orsay, France; and §Department of Chemistry, University of Arizona, Tucson, Arizona 85721

Received July 26, 2000; in revised form November 28, 2000

The electronic spectra of CuCl were observed in the 18 000 cm^{-1} to 25 000 cm^{-1} spectral region using a Bruker IFS 120 HR Fourier transform spectrometer (FTS) and with the FTS associated with the McMath-Pierce Solar Telescope at Kitt Peak. On the basis of *ab initio* calculations, the labels for the electronic states were revised, and the $a^3\Sigma_1^+–X^1\Sigma^+$ 0–0 band, the $b^3\Pi_0–X^1\Sigma^+$ 0–0, 1–0, and 0–1 bands, the $b^3\Pi_1–X^1\Sigma^+$ 0–0, 1–0, and 0–1 bands, the $A^1\Pi–X^1\Sigma^+$ 0–0, 1–0, and 0–2 bands, and the $B^1\Sigma^+–X^1\Sigma^+$ 0–0 and 1–0 bands were measured. Improved spectroscopic constants were obtained for the excited and ground states.

INTRODUCTION

A simple model for the electronic states of CuCl is to consider the molecule as a Cu^+ ($3d^{10}$) cation and a Cl^- ($3p^6$) anion, and the molecular orbitals in terms of the atomic orbitals of the individual ions. Using this model, the 3*p* orbitals on the chlorine form a closed subshell and the lower energy electronic transitions can be attributed to an electron being promoted from one of the filled 3*d* orbitals to the empty 4*s* orbital on the copper ion. When this happens, the electron leaves behind a "*d*-hole" which results in three possible states: Σ, Π, and Δ. The state depends on which orbital the electron was promoted from, d_{z^2}, $d_{xz\ or\ yz}$, or $d_{xy\ or\ x^2-y^2}$ for Σ, Π, or Δ, respectively. Each of the resultant states can also be either a singlet or a triplet. Thus, CuCl has a $X^1\Sigma^+$ ground state and six low-lying excited states, $^1\Sigma^+$, $^3\Sigma^+$, $^1\Pi$, $^3\Pi$, $^1\Delta$, and $^3\Delta$.

The first analyses of CuCl in 1927 (*1*) and 1938 (*2*) were vibrational analyses that located five low-lying electronic states. The five band systems were the result of transitions with a common lower state. Since then, rotational analyses of the electronic emission bands have been performed (*3–7*), as well as work in the millimeter and microwave regions of the spectrum (*8, 9*). Work performed by Rao *et al.* (*4, 5*), as well as contributions by Lagerqvist and Lazarava-Girsamoff (*10*) and Ahmed and Barrow (*11*), led to the characterization of the six excited electronic states, originally labeled as $A^1\Pi$, $B^1\Pi$, $C^1\Sigma^+$, $D^1\Pi$, $E^1\Sigma^+$, and $F^1\Pi$ states. However, the first reference to a triplet state was not made until 1984, when Balfour and Ram attributed a 13 500 cm^{-1} band to a $^3\Sigma–^1\Sigma$ transition by analogy with a similar transition in CuF (*12, 13*). It now appears that this transition is between two highly excited electronic states (*14*). *Ab initio* calculations were performed with new assignments for the electronic systems that included triplet states (*15, 16*). Delaval *et al.* measured the radiative lifetimes of the low-lying electronic excited states and also suggested that some of the singlet states of CuCl were in fact triplet states (*17*).

Recent work on CuCl includes microwave experiments in the ground and first excited vibrational levels (*18, 19*), laser excitation spectroscopy of the 0–0 bands of the $D^1\Pi–X^1\Sigma^+$ and $E^1\Sigma^+–X^1\Sigma^+$ transitions (*20, 21*), and *ab initio* calculations (*22–25*).

EXPERIMENTAL DETAILS

To obtain an electronic emission spectrum of CuCl, a copper hollow cathode lamp was used. The lamp consisted of a stainless steel chamber as the anode and a copper hollow cathode with an inner diameter of 1 cm.

The initial experiment was run with a small sample of Cu metal inside the lamp, which was operated with HCl and He gas. Emission from the CuCl from inside the cathode was focussed with a lens into a Bruker IFS 120 HR Fourier transform spectrometer, modified to obtain double-sided interferograms, located at the University of Waterloo. To increase the signal-to-noise ratio, the experiment was improved. CuCl powder and Cu metal were placed inside the lamp, which was then operated with only He gas at a pressure of 5 Torr. The lamp was operated at a current of 200 to 250 mA.

The spectrum was recorded in two spectral regions at a resolution of 0.02 cm^{-1} to cover the total spectral range from 18 000 to 26 500 cm^{-1} with a photomultiplier tube (PMT) detector and a visible quartz beamsplitter. Bandpass filters were inserted to reduce the effect of strong atomic lines on the spectrum.

Supplementary data for this article are available on IDEAL (http://www.indealibrary.com) and as part of the Ohio State University Molecular Spectroscopy Archives (http://msa.lib.ohio-state.edu/jmsa_hp.htm).

0022-2852/01 $35.00

In the first spectrum, spanning the region from 18 000 to 23 000 cm^{-1}, a 550-nm blue pass filter and a 450-nm red pass filter were used. The second spectrum, spanning the region from 20 000 to 26 500 cm^{-1}, was recorded using a 450-nm blue pass filter and a 400-nm red pass filter.

The excited CuCl molecules were also produced in a King-type carbon tube furnace, charged with approximately 10 g of CuCl powder. The tube was filled with 50 Torr of helium, then heated to 1900°C, with a final pressure of 400 torr. The CuCl emission was focused onto the entrance aperture of the Fourier transform spectrometer (FTS), located at the McMath–Pierce Solar Observatory, Kitt Peak, Arizona. Twenty scans at a resolution of 0.021 cm^{-1} were co-added in 65 minutes of integration in 3rd-order alias. The spectral region from 22 200 to 33 000 cm^{-1} was recorded by the FTS, which was configured with a $CuSO_4$ filter, a quartz beamsplitter, and two midrange diode detectors. The carbon furnace gave spectra with higher rotational excitation than the hollow cathode lamp.

CuCl SPECTRAL ANALYSIS

The CuCl spectra obtained from the Waterloo experiments are shown in Figs. 1 and 2. Rovibronic line positions were measured for the $a^3\Sigma_1^+–X^1\Sigma^+$ 0–0 band, the $b^3\Pi_0–X^1\Sigma^+$ 0–0, 1–0, and 0–1 bands, the $b^3\Pi_1–X^1\Sigma^+$ 0–0, 1–0, and 0–1 bands, the $A^1\Pi–X^1\Sigma^+$ 0–0, 1–0, and 0–2 bands, and the $B^1\Sigma^+–X^1\Sigma^+$ 0–0, and 1–0 bands. Figure 3 shows the 0–0 band of the $B^1\Sigma^+–X^1\Sigma^+$ transition. For the more intense bands, strong unblended lines were measured to an estimated precision of ±0.005 cm^{-1}. However, nearly all of the observed line positions were blended and therefore the estimated precision varied from ±0.02 to ±0.04 cm^{-1}. This severe blending made the rotational analysis difficult.

TABLE 1
The Low-Lying Electronic States of CuCl

Previous Label	Current Label
$A\,^1\Pi$	$a\,^3\Sigma_1^+$
$B\,^1\Pi$	$b\,^3\Pi_1$
$C\,^1\Sigma^+$	$b\,^3\Pi_0$
$D\,^1\Pi$	$A\,^1\Pi$
$E\,^1\Sigma^+$	$B\,^1\Sigma^+$
$F\,^1\Pi$	$c\,^3\Delta_1$

The electronic band systems were labeled based on the presence of a Q branch in the bands, as well as on comparisons with previous assignments that are based on radiative lifetime studies (*26*) and *ab initio* calculations (*24*). The selection rule for Ω is $\Delta\Omega = 0, \pm 1$. Those transitions that have a Q branch have $\Omega = 1$ in the excited state, while those without a Q branch have $\Omega = 0^+$. The multiplicity and Λ values were then determined by the lifetime studies and the *ab initio* calculations. The new labels for the low-lying electronic states are listed in Table 1. The presence of triplet-to-singlet transitions, forbidden by Hund's case (a) selection rules, suggests that there is considerable mixing of the triplet and singlet states. For example, the presence of a Q branch and substantial "effective lambda doubling" in the $a^3\Sigma_1^+–X^1\Sigma^+$ system further suggests that mixing occurs between the $a^3\Sigma_1^+$ and $A^1\Pi$ states.

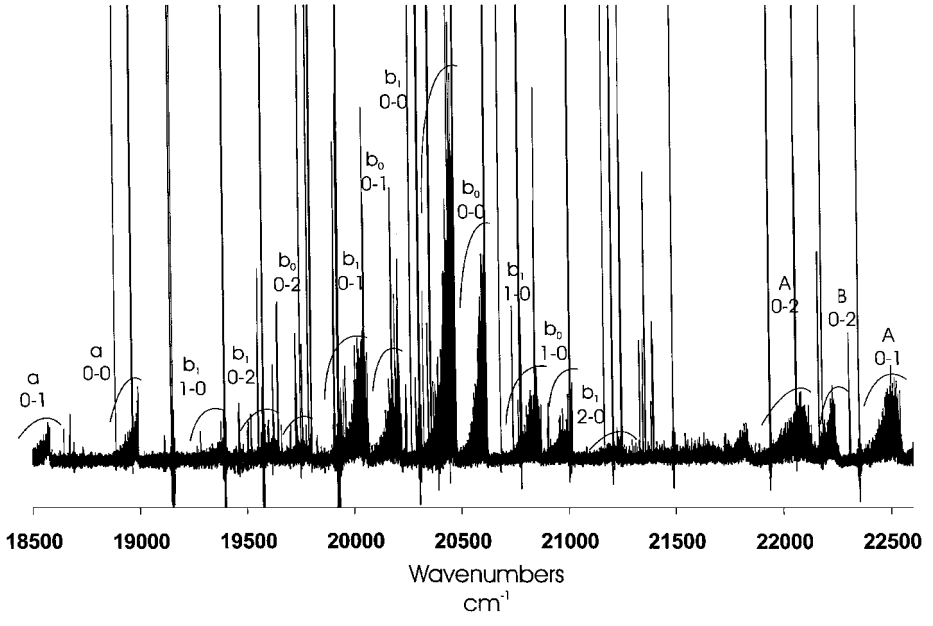

FIG. 1. The emission spectrum of CuCl, spanning the spectral region from 18 500 to 22 500 cm^{-1}. a, b_0, b_1, A, and B indicate the $a^3\Sigma_1^+–X^1\Sigma^+$, $b^3\Pi_0–X^1\Sigma^+$, $b^3\Pi_1–X^1\Sigma^+$, $A^1\Pi–X^1\Sigma^+$, and $B^1\Sigma^+–X^1\Sigma^+$ transitions, respectively.

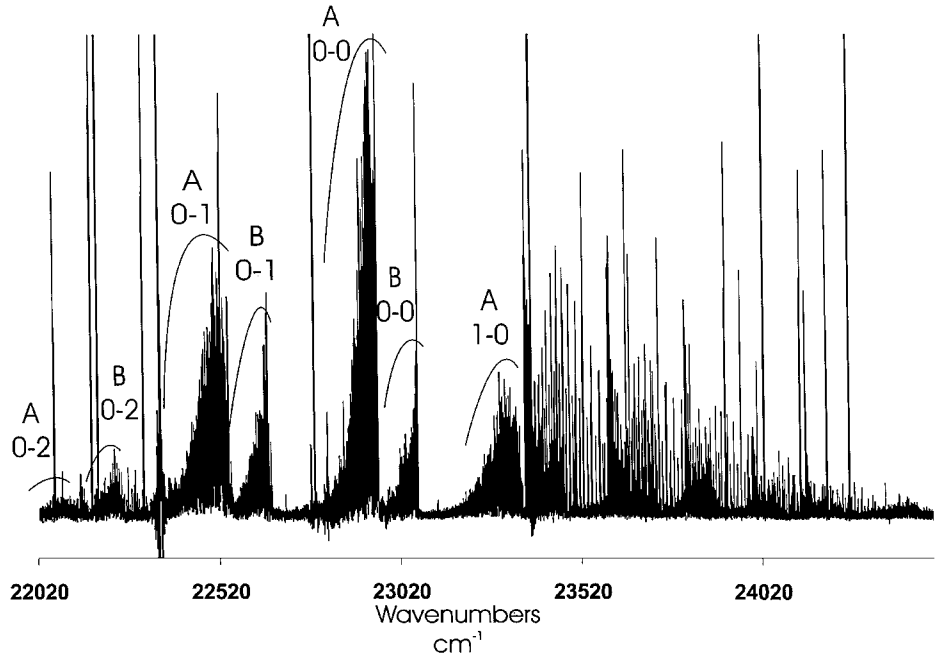

FIG. 2. The emission spectrum of CuCl, spanning the spectral region from 22 000 to 24 500 cm^{-1}. A and B indicate the $A^1\Pi$–$X^1\Sigma^+$ and $B^1\Sigma^+$–$X^1\Sigma^+$ transitions, respectively.

The 1640 measured line positions for $^{63}Cu^{35}Cl$ are provided in the *JMS* depository. The signal-to-noise ratio for the strongest lines was better than 25. The line positions were measured using the PC Decomp program and then arranged into series of *P*, *Q*, and *R* branches for each individual band using a color Loomis–Wood program.

A spectrum containing Ar and He lines was obtained for the calibration of the CuCl lines. The He line positions were first calibrated using the Ar line positions from Ref. (*27*). The He lines present in both the CuCl spectrum and the Ar and He spectrum were then used to obtain a calibration factor for the calibration of the CuCl line positions.

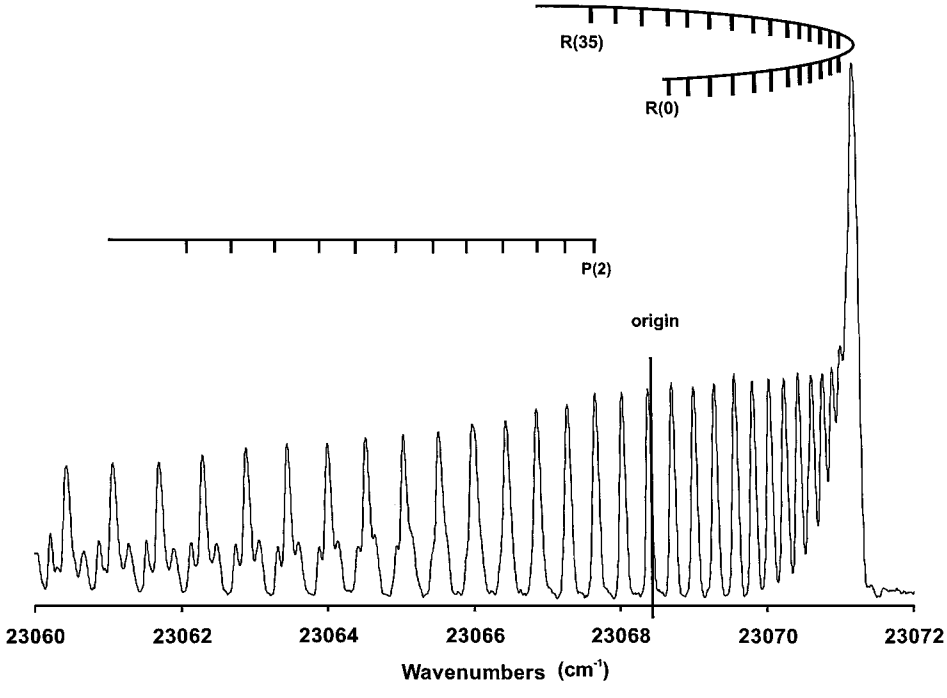

FIG. 3. The 0–0 band of the $B^1\Sigma^+$–$X^1\Sigma^+$ transition.

TABLE 2
Band Constants for $^{63}Cu^{35}Cl$ (in cm^{-1})

Electronic State	v	T_v	B_v	$10^7 D_v$	$10^{13} H_v$	$10^3 q_v$	$10^8 q_{Dv}$
$X\,^1\Sigma^+$	0	---	0.177741295(5)	1.29803(10)	-0.437(57)	---	---
	1	414.4036(11)	0.176732222(16)	1.29748(13)	-0.437[a]	---	---
	2	825.5775(14)	0.175727053(11)	1.296518(87)	-0.437[a]	---	---
$a\,^3\Sigma_1^+$	0	18994.4559(15)	0.1701872(19)	1.1616(39)	-2.33(16)	-4.0595(29)	0.432(61)
$b\,^3\Pi_1$	0	20476.0848(12)	0.1697742(11)	1.2581(22)	1.33(13)	-0.7008(17)	0.699(40)[b]
	1	20874.3732(20)	0.1683756(56)	1.2943(43)	1.33[a]	-1.586(10)	0.699[a, c]
$b\,^3\Pi_0$	0	20621.8403(10)	0.17049768(90)	1.2426(18)	-0.56(11)	---	---
	1	21017.9324(17)	0.1695968(32)	1.264(12)	-0.564[a]	---	---
$A\,^1\Pi$	0	22958.4771(13)	0.1688527(16)	1.3272(45)	-0.683(70)	-1.1191(26)	-1.458(86)
	1	23349.9875(16)	0.167887(12)	1.95(13)	-0.683[a]	-1.087(24)	-13.7(27)
$B\,^1\Sigma^+$	0	23068.2615(29)	0.1676150(51)	0.943(22)	-4.1(24)	---	---
	1	23470.4926(31)	0.1664998(52)	1.031(21)	4.1(22)	---	---

[a] fixed.
[b] $q_{Hv} = 4.18(22) \times 10^{-13}$ cm^{-1}.
[c] $q_{Hv} = 4.18 \times 10^{-13}$ cm^{-1}, held constant.

The data were then fitted to the energy level expression

$$E_{v,j} = T_v + \left[B_v \pm \frac{q_v}{2}\right] J(J+1) - \left[D_v \mp \frac{q_{D_v}}{2}\right] [J(J+1)]^2 + \left[H_v \pm \frac{q_{H_v}}{2}\right] [J(J+1)]^3 + \cdots, \quad [1]$$

where T_v includes the electronic and vibrational energy, B_v, D_v, and H_v are the usual band constants, and q_v and q_{Dv} are the lambda-doubling constants. Initial fits for individual bands were performed by fixing the ground electronic state constants to literature values obtained from pure rotational transitions (*8, 18, 19*). A final fit was performed with all the data, including the microwave data from the literature, and the excited and ground state constants were allowed to float. The constants obtained are listed in Table 2.

The equilibrium molecular constants, listed in Table 3, were determined using the expression for the energy of a transition between vibrational levels characterized by $v+1$ and v of an anharmonic diatomic oscillator,

$$\Delta G_{v+1/2} = G(v+1) - G(v) = \omega_e - 2\omega_e x_e - 2\omega_e x_e v + \cdots, \quad [2]$$

and the parametric expression describing the vibrational dependence of the rotational constants,

$$B_v = B_e - \alpha_e\left(v + \frac{1}{2}\right) + \gamma_e\left(v + \frac{1}{2}\right)^2 + \cdots. \quad [3]$$

For the $b^3\Pi_0$, $b^3\Pi_1$, $A^1\Pi$, and $B^1\Sigma^+$ states, $\Delta G_{1/2}$ values are shown in place of ω_e, as only two vibrational levels were measured. Note that the band with $\Delta v \neq 0$ are much more complex than the 0–0 bands and there is the possibility of error in the numbering of the P and R branches.

A comparison of the T_v value obtained for the $B^1\Sigma^+$–$X^1\Sigma^+$ 0–0 transitions with that from Ref. (*21*) shows agreement within 0.004 cm^{-1}, which is less than the linewidth obtained for our

TABLE 3
Molecular Equilibrium Constants for $^{63}Cu^{35}Cl$ (in cm^{-1})

Electronic State	ω_e	$\omega_e x_e$	B_e	$10^3 \alpha_e$	r_e (Å)
$X\,^1\Sigma^+$	417.6405(25)	1.6173(25)	0. 178247296(77)	1.012950 (77)[a]	1.22576663(53)
$a\,^3\Sigma_1^+$	---	---	[0.1701872(19)][b]	---	1.254457(14)[d]
$b\,^3\Pi_1$	398.2884(32)[c]	---	0.1704735(67)	1.3986(67)	1.253403(49)
$b\,^3\Pi_0$	396.0921(27)[c]	---	0.1709481(41)	0.9009(41)	1.251662(30)
$A\,^1\Pi$	391.5104(29)[c]	---	0.169336(14)	0.966(14)	1.25761(10)
$B\,^1\Sigma^+$	402.2311(60)[c]	---	0.1681726(103)	1.1152(103)	1.261949(77)

[a] $\gamma_e = 1.952(77) \times 10^{-6}$ cm^{-1}.
[b] B_0.
[c] $\Delta G_{1/2}$.
[d] r_0.

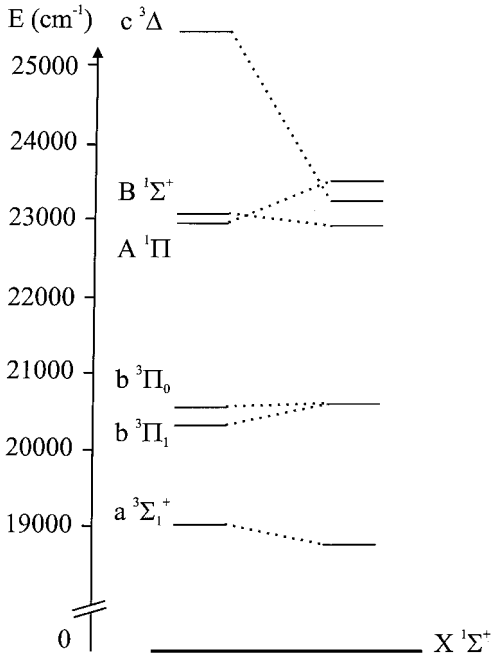

FIG. 4. Energy level diagram of the low-lying electronic states of CuCl. The left side shows the experimental values obtained in this work. The $^3\Delta$ transition energy was taken from Ref. (*26*). The right side shows recent theoretical results (*24*).

CuCl spectra. The $A^1\Pi$–$X^1\Sigma^+$ 0–0 band of the $^{63}Cu^{37}Cl$ isotopomer was also measured by the same group and T_0 was determined for the dominant isotopomer, $^{63}Cu^{35}Cl$, by isotopic scaling. The value obtained agrees with our determination of T_0 within 0.015 cm^{-1}.

Figure 4 shows the energy level diagram of the electronic states of CuCl. The left side shows the T_v values obtained during this work. For comparison, the right side shows the most recent theoretical values (*24*). While the theoretical results do not show the spin-orbit splitting in the $^3\Pi$ state, as observed in our experiment, there is good agreement between the T_v values within 500 cm^{-1}. The $^3\Delta$ state shown in Fig. 4 was not measured in this work. The value shown was taken from Ref. (*26*) and included for completeness.

The effective Λ-doubling constant, q, for the $a^3\Sigma_1^+$ state was determined with good precision; $-4.059(29) \times 10^{-3}$ cm^{-1}, and the previous positive value (*6*) is clearly erroneous. In the a state, the "Λ-doubling" effect is mainly due to the spin–spin interaction in the triplet state, which is in fact a second order spin–orbit effect (*28*). By using Hund's case (a) basis functions and ignoring centrifugal distortion terms, the rotational energy levels for the $a^3\Sigma_1^+$ state are given by the approximate formulae

$$E(\Omega = 1^-) = BJ(J+1) - \gamma + \frac{2}{3}\lambda, \quad [4]$$

$$E(\Omega = 0^+) = BJ(J+1) - qJ(J+1) + 2B - 2\gamma - \frac{4}{3}\lambda, \quad [5]$$

$$E(\Omega = 1^+) = E(\Omega = 1^-) + qJ(J+1). \quad [6]$$

In this approximation, B, γ, and λ are the rotational, spin–rotation, and spin–spin constants, respectively, and the spin–spin constant is assumed to be large ($\lambda \gg 2BJ$). The value of q is then given by the formula

$$q = \frac{(\gamma - 2B)^2}{2\lambda + \gamma - 2B}. \quad [7]$$

From Eq. [7] (ignoring the spin–rotation constant), the spin–spin constant is estimated to be -14 cm^{-1}. The $a^3\Sigma_{0^-}^+$ state, expected in the region 28 cm^{-1} below the $a^3\Sigma_1^+$ state, was not observed.

The Λ-doubling splitting in a $^1\Pi$ state is usually explained by a simple pure precession approximation (*28*):

$$q_v = \sum_{v'} \frac{2[\langle B^1\Sigma, v'|B(r)\mathbf{L}^-|A^1\Pi, v\rangle]^2}{E_{A,v'} - E_{B,v}} \approx \frac{2l(l+1)B_v^2}{E_{A,v} - E_{B,v}}. \quad [8]$$

For $l = 2$, however, the calculated q_0 is -3.1×10^{-3} cm^{-1}, which is three times larger than the observed value, $-1.1191(26) \times 10^{-3}$ cm^{-1}.

A similar discrepancy was also seen in the $b^3\Pi_1$ state. In this case, the splitting between e and f levels is represented by the formula (*29*)

$$E_f - E_e = \left\{ q^* + \frac{4B^*(p^* + 2q^*)}{A^* - 2\lambda^*} \right\} J(J+1), \quad [9]$$

where the constants denoted with asterisks indicate "true" molecular constants for the $^3\Pi$ state obtained with Hund's case (a) basis functions and the $\mathbf{N}^2$ Hamiltonian defined in Ref. (*30*). Assuming that the spin–orbit and spin–spin coupling constants, A^* and λ^*, are similar to those of CuF, 413 cm^{-1} and -18 cm^{-1}, respectively (*31*), the Λ-doubling constant is expected to be close to $-q^*$ in Eq. [9], and thus,

$$-q_v \approx q^* = \sum_{v'} \frac{2[\langle a^3\Sigma, v'|B(r)\mathbf{L}^-|b^3\Pi, v\rangle]^2}{E_{b,v} - E_{a,v'}}$$

$$\approx \sum_{v'} \frac{2l(l+1)[\langle a^3\Sigma, v'|B(r)|b^3\Pi, v\rangle]^2}{E_{b,v} - E_{a,v'}} \quad [10]$$

within the pure precession approximation. The value of $q_0(-q^*)$ from this formula was calculated as -2.3×10^{-3} cm^{-1}, which is three times smaller than the observed value of $-7.008(17) \times 10^{-3}$ cm^{-1}. Moreover, higher order Λ-doubling terms were required in the fit, which is unlikely for a heavy molecule in a normal $^1\Pi$ state. There is probably a similar effect in CuF, in which the e–f splitting is not proportional to $J(J+1)$ (*32, 33*) because the $b^3\Pi_{0^+}$ state is located only 55 cm^{-1} higher than the $b^3\Pi_1$ state (*34*).

The simple-minded pure precession mixing is compromised primarily by configuration mixing and spin–orbit coupling. A more sophisticated model that includes these effects has been developed by Delaval *et al.* (*35*). Their predictions for the q's

are -5.0×10^{-3}, -1.04×10^{-3}, and -2.1×10^{-3} cm^{-1} for the $a^3\Sigma_1^+$, $b^3\Pi_1$, and $A^1\Pi$ states, respectively, to be compared with the observed values (Table 2) of -4.06×10^{-3}, -0.70×10^{-3} and -1.12×10^{-3} cm^{-1}. This model is obviously much better than pure precession but still deviates somewhat from experiment.

CONCLUSIONS

The emission spectra of CuCl have been investigated at high resolution in the region from 18 000 to 25 000 cm^{-1} using a Fourier transform spectrometer. The bands observed in this region have been assigned to a number of transitions involving electronic states with recently revised labels. Rotational analysis of these transitions has been carried out and improved spectroscopic constants have been obtained for the excited and ground electronic states.

ACKNOWLEDGMENTS

This work was supported by the Natural Sciences and Engineering Research Council of Canada. We also acknowledge the Petroleum Research Fund and the Killam Foundation for partial support. LCO gratefully acknowledges support from the National Science Foundation, NSF-CHE-9753254. ME acknowledges support from CNRS/GDR of Physico-Chimie des Grains et Molecules Interstellaires.

REFERENCES

1. R. Ritschl, *Z. Phys*. **42,** 172–210 (1927).
2. S. Bloomenthal, *Phys. Rev*. **54,** 498–497 (1938).
3. J. Terrien, *Ann. Phys. NY* **9,** 477–538 (1938).
4. P. R. Rao and J. K. Brody, *J. Chem. Phys.* **35,** 776–787 (1961).
5. P. R. Rao, R. K. Asundi, and J. K. Brody, *Can. J. Phys.* **40,** 412–422, 423–430, and 1443–1456 (1962).
6. G. P. Mishra, S. B. Rai, and K. N. Upadhya, *Can. J. Phys.* **59,** 289–297 (1981).
7. P. M. R. Rao, *Indian J. Pure Appl. Phys.* **18,** 200–203 (1980).
8. E. L. Manson, F. C. De Lucia, and W. Gordy, *J. Chem. Phys.* **62,** 1040–1043 (1975).
9. E. Tiemann and J. Hoeft, Z. *Naturforsch.* **32a,** 1477–1479 (1977).
10. A. Lagerqvist and V. Lazarava-Girsamoff, *Ark. Fys.* **20,** 543–553 (1961).
11. F. Ahmed and R. F. Barrow, *J. Phys. B Ato. Mol. Phys.* **8,** L362–L363 (1975).
12. W. J. Balfour and R. S. Ram, *J. Phys. B Ato. Mol. Phys.* **17,** L19–L21 (1984).
13. W. J. Balfour and R. S. Ram, *J. Phys. B Ato. Mol. Phys.* **16,** L163–L166 (1983).
14. L. C. O'Brien, H. Cao, and J. J. O'Brien, *J. Mol. Spectrosc.* **199,** 100–108 (2000).
15. N. W. Winter and D. L. Huestis, *Chem. Phys. Lett.* **133,** 311–316 (1987).
16. M. T. Nguyen, M. A. McGinn, and N. J. Fitzpatrick, *J. Chem. Soc. Faraday Trans. 2* **82,** 1427–1443 (1986).
17. J. M. Delaval, Y. Lefebvre, H. Bocquet, P. Bernage, and P. Niay, *Chem. Phys.* **111,** 129–136 (1987).
18. R. J. Low, T. D. Varberg, J. P. Connelly, A. R. Auty, B. J. Howard, and J. M. Brown, *J. Mol. Spectrosc.* **161,** 499–510 (1993).
19. K. D. Hensel, C. Styger, W. Jager, A. J. Merer, and M. C. Gerry, *J. Chem. Phys.* **99,** 3320–3328 (1993).
20. A. Bath and E. Tiemann, *Chem. Phys. Lett.* **175,** 84–86 (1990).
21. I. Burghardt, L. R. Zink, D. A. Fletcher, J. M. Brown, and I. R. Beattie, *Mol. Phys.* **67,** 1401–1417 (1989).
22. A. Ramirez-Solis and J. P. Daudey, *J. Phys. B Ato. Mol. Phys.* **23,** 2277–2291 (1990).
23. A. Ramirez-Solis, *Phys. Rev. A.* **47,** 1510–1513 (1993).
24. C. Sousa, W. A. De Jong, R. Broer, and W. C. Nieuwpoort, *J. Chem. Phys.* **106,** 7162–7169 (1997).
25. C. Sousa, W. A. De Jong, R. Broer, and W. C. Nieuwpoort, *Mol. Phys.* **92,** 677–686 (1997).
26. J. M. Delaval, J. Schamps, A. Ramirez-Solis, and J. P. Daudey, *J. Chem. Phys.* **97,** 6588–6592 (1992).
27. G. Norlén, *Phys. Scripta*, **8,** 249–268 (1973).
28. H. Lefebvre-Brion and R. W. Field, "Perturbations in the Spectra of Diatomic Molecules." Academic Press, Orlando, FL., 1986.
29. J. M. Brown and A. J. Merer, *J. Mol. Spectrosc.* **74,** 488–494 (1979).
30. J. M. Brown, E. A. Colbourn, J. K. G. Watson, and F. D. Wayne, *J. Mol. Spectrosc.* **74,** 294–318 (1979).
31. C. R. Brazier, J. M. Brown, and T. C. Steimle, *J. Mol. Spectrosc.* **97,** 449–453 (1983).
32. F. Ahmed, R. F. Barrow, A. H. Chojnicki, C. Dufour, and J. Schamps, *J. Phys. B* **15,** 3801–3818 (1982).
33. T. C. Steimle, C. R. Brazier, and J. M. Brown, *J. Mol. Spectrosc.* **110,** 39–52 (1985).
34. J. M. Delaval, J. Schamps, and C. Dufour, *J. Mol. Spectrosc.* **137,** 268–277 (1989).
35. J. M. Delaval, J. Schamps, and F. L. Sefyani, *Phys. Scrip.* **49,** 404–407 (1994).